Spatially conserved pathoprotein profiling in the human suprachiasmatic nucleus in progressive Alzheimer's disease stages

Author information

Gowoon Son, PhD[1], Mihovil Mladinov, MD, PhD[1], Felipe Luiz Pereira, PhD[1], Song Hua Li, BS[1], Chia-Ling Tu, PhD[2], Grace Judge[1], Yumi Yang, BA[1], Claudia Kimie Suemoto, MD, PhD, MSc[3,4], Renata Elaine Paraízo Leite, BPT, PhD[3,5], Vitor Paes[5,] , Carlos A. Pasqualucci[3,5], Wilson Jacob-Filho[4], Salvatore Spina, MD, PhD[1], William W. Seeley, MD[1], Wenhan Chang, PhD[2], Thomas Neylan, MD[1,6] and Lea T. Grinberg, MD, PhD[1,3,5]
(1) Memory and Aging Center, UCSF Weill Institute for Neurosciences, University of California, San Francisco, San Francisco, CA, USA,
(2) San Francisco VA Medical Center, UCSF, San Francisco, CA, USA,
(3) Physiopathology in Aging Laboratory (LIM-22), Department of Internal Medicine, University of São Paulo Medical School, São Paulo, Brazil.
(4) Division of Geriatrics, Department of Internal Medicine, University of São Paulo Medical School, São Paulo, Brazil
(5) Department of Pathology, University of Sao Paulo Medical School, Sao Paulo, Brazil.
(6) Department of Psychiatry, University of California, San Francisco, San Francisco, CA, USA

Abstract

Individuals with Alzheimer's Disease (AD) experience circadian rhythm disorder. The circadian rhythm is synchronized by a master clock, the suprachiasmatic nucleus (SCN), which is a tiny hypothalamic nucleus. Little is known about the molecular and pathological changes that occur in the SCN during AD progression. We examined postmortem brains of 12 controls without AD neuropathological changes (Braak stage (Braak)0) and 29 subjects at progressive ADNC stages. To investigate potential AD-specific changes, we measured the neuronal counts of arginine vasopressin (AVP) and vasoactive intestinal peptide (VIP) positive neurons, along with the ADNC burden in the SCN. We investigated in adjacent hypothalamic nuclei which are also composed of AVP+ neurons but show more resilience to AD: supraoptic nucleus (SON) and paraventricular nucleus (PVN). To understand the pattern of protein dysregulation associated to AD progression, we performed in-situ proteomics, including probes for 39 proteins commonly dysregulated in AD, using GeoMx Digital Spatial Profiling (DSP) in the three nuclei (total of 703 area of interests (AOIs)). Neurofibrillary tangles were found selectively in SCN. We failed to detect neurofibrillary tangles (NFTs) in SON, only a mild dysregulation of p-tau at Braak VI in PVN and SON. Additionally, the SCN showed increases in glial proteins already in Braak I, whereas these proteins remained unaltered in the other nuclei. The SCN is vulnerable to AD-tau pathology and show immune dysregulation even at Braak I but is protected against ß-amyloid (Aß) accumulation. This vulnerability pattern in SCN supports the idea that SCN dysfunction contributes to circadian rhythm disturbances in AD, a phenomenon observed even in the stage before the onset of cognitive disorder.

Introduction

Circadian rhythm disorders are investigated as an early symptom in patients with Alzheimer's disease (AD). The circadian rhythm is a roughly 24-hour biological rhythm that regulates cellular metabolism in the brain, maintaining a balance between synthesis and degeneration. A Suprachiasmatic nucleus (SCN) plays a vital role in regulating and synchronizing neuronal and glial circadian rhythm therefore is called a central circadian pacemaker in the human brain (1). The SCN is a hub of processing molecular and environmental circadian information, has a direct connection to various hypothalamic nuclei and the brainstem nuclei, which initiates an accumulation of the neurofibrillary tangle (NFT) in the progression of AD (2,3). Therefore, SCN integrity is fundamental for assessing circadian abnormalities dependent on disease progression. However, previous neuropathological examinations investigating abnormal circadian behavior have been limited in the SCN, while primarily focused on the hippocampal formation and cortical areas. These regions are known to be involved in pathological alterations in the severe stages of AD (4,5).

Hence, to examine the extent to which the SCN is pathologically involved in the progression of AD, we utilized the anatomical and physiological features of the SCN. The human SCN, a tiny nucleus composed of 50,000 neurons in a hemisphere of the anterior hypothalamus, exhibits variability in morphology between individuals (6,7). The SCN signals are transferred by neuromodulatory cells, which are spatially organized in their expression within the SCN (8). Among 10 types of the different SCN neuromodulatory cells, arginine vasopressin (AVP) and vasoactive intestinal peptide (VIP), each is in the shell and core of the SCN, respectively. AVP cells are known for transferring the efferent signal from the SCN to the PVN and other hypothalamic nuclei, in contrast, VIP cells receive the afferent signals from the retinal ganglion cells and the subcortical area such as raphe nuclei, thalamic intergeniculate leaflet, and parabrachial nucleus in the brainstem (1).

We conducted in-situ proteomics in the human postmortem SCN at progressive stages of AD neuropathological change (ADNC), employing barcode-conjugated antibodies for 39 proteins commonly dysregulated in AD. We utilized GeoMx Digital Spatial Profiling (DSP), which enables quantification of the spatially conserved protein expression. The digitally examined differentially expressed proteins (DEPs) were validated through neuropathological examination to investigate the accumulation of the insoluble form of AD-related proteins. For regional control, we investigated the neighboring anterior hypothalamic nuclei, which are also composed of AVP+ neurons but show more resilience to AD: the supraoptic nucleus (SON) and paraventricular nucleus (PVN).

Materials and methods

Participants and neuropathological diagnosis

Participants were recruited from the Neurodegenerative Disease Brain Bank (NDBB) from Memory and Aging Center of the University of California, San Francisco (San Francisco, USA), until 2023, and Brazilian BioBank for Aging Studies (BBAS) from the university of São Paulo Medical School (São Paulo, Brazil), until 2023. BBAS are population-based and host a high percentage of control subjects who are not available in NDBB. A total of 11 patients with amnestic AD (Braak VI), 30 cognitively normal and neuropathologically confirmed individuals (12 Braak 0, 12 Braak I, and 6 Braak II). All neurological and neuropathological assessments were performed using standardized protocols and followed the internationally accepted criteria for neurodegenerative diseases (4,5). Exclusion criteria were absence of any other significant neurodegenerative or cerebrovascular changes. Table 1 indicates demographic information of the participants.

Postmortem specimen processing

Specimen processing was followed by the UCSF NDBB Neuropathological assessment protocol. Human hypothalamus was collected after fixation in 10% neutral buffered formalin, and was processed and embedded in paraffin, cut into 6um thick sections, and mounted on glass slides. Region-of-interests (ROIs) were identified using Allen Brain Atlas (Allen Institute for Brain Science), human hypothalamus atlas (9), and AVP/VIP RNA probe expression using fluorescent In-situ hybridization (FISH).

Multiplex fluorescent In-situ hybridization (FISH) combined with immunofluorescence

Specimen sections were deparaffinized in xylene for 30min, washed in 100%, 95%, and 80% ethanol. To run the FISH assay, followed the instruction in the user manuals Formalin-Fixed Paraffin-Embedded (FFPE) Sample Preparation and Pretreatment and the RNAscope Multiplex Fluorescent Reagent Kit v2 (Cat. No. 323100, Advanced Cell Diagnostics, Newark, CA, USA). A summarized tissue pretreatment and probe binding procedure is following. Incubate the slides in hydrogen peroxide, perform target retrieval with a standard protocol, apply protease Plus, incubate probes AVP-C2 (Cat. No. 401361-C2), VIP-C3 (Cat. No. 452751-C3). RNA signals are amplified and bound fluorophores, Opal 570 for AVP-C2 and Opal 650 for VIP-C3. Slides are incubated in Sudan Black B solution to avoid autofluorescent signals.

Digital spatial profiling with the GeoMx Human protein panels

The slides with the AVP and VIP RNA probes were processed by the GeoMx TM Digital Spatial Profiler slide preparation protocol (NanoString Technologies, Seattle, WA, USA). After an antigen retrieval with 1x citrate buffer and a blocking step with Buffer W, the slides are incubated with GeoMx Human Protein Modules for nCounter (Alzheimer's Pathology Panel (Cat. No. 121300109), Alzheimer's Pathology Extended Panel (Cat. No. 121300114), Neural Cell Profiling Panel (Cat. No. 121300108), Autophagy Panel (Cat. No. 121300115), NanoString Technologies, Seattle, WA, USA), CaSR (MAb 1C12D7), metabotropic gamma-aminobutyric acid (GABA) receptors GABBR1 (Abcam, ab264069, RabMAb EPR22954-47), and GABBR2 (Abcam, ab230136, RabMAb EP2411), and Alexa Fluor 594 (AF594) (Cat. No. A20182, Thermo

Fisher Scientific)-conjugated AT8 (phosphor-tau, S202, and T205) (Cat. No. MN1020, Thermo Fisher Scientific) and GFAP (Cat. No.NBP1-05197AF594, Novus Biologicals) antibody. The slides were treated by 4% paraformaldehyde for a post-fixation and were stained by SYTO 13 (Cat. No. S7575, Thermo Fisher Scientific) for nuclei staining.

The slides were scanned using the GeoMx Digital Spatial Profiler (DSP) instrument at 20x magnification. The morphology of the hypothalamus nuclei (SCN, PVN, and SON) were visualized using FISH-labeled AVP and VIP probes. NFTs were labeled with AF594-conjugated AT8 antibody. Area-of-interest were selected using freeform segmentation with a size, maximum 660 μM^2. Segmentation was performed based on human hypothalamus anatomy and physiological markers and morphological characteristics of each nucleus. Multiple sections (2~4 sections per case) were analyzed for an unbiased DSP analysis. Total 703 of AOIs were collected.

GeoMx DSP protein nCounter quantification

The oligonucleotide tags corresponding to bound antibodies within each cell compartment were released by UV (385 nm wavelength) photocleavage. The released oligonucleotides were recovered and dispensed into 96-well plates. The indexing oligonucleotides were dried down and resuspended in diethyl pyrocarbonate (DEPC)-treated water, hybridized to 4-color, 6-spot optical barcodes, and digitally counted using the nCounter system (NanoString Technologies, Seattle, WA, USA).

Differentially expressed protein analysis of human GeoMx DSP data and statistics

Raw data was exported using GeoMx DSP software to normalize the digital counts using internal spike-in controls (ERCCs) and scale each AOIs to area. All batch control, post-normalization, statistical analysis, and differentially expressed protein (DEP) data visualization were performed using R software (ver. 4.3.1, R Foundation for Statistical Computing, Vienna, Austria, https://www.R-project.org/).

Histological quantification and statistics

The number of cells and the size of ROIs were estimated at a series of sections spanning the whole SCN using Stereo Investigator probe (ver. 2023, MBF Bioscience LLC, Williston, VT, USA). The scanned images of histological slides that underwent GeoMX DSP analysis were loaded into the Stereo Investigator software and were used to quantify the number of AVP+ and VIP+ neurons. Two Braak 0 and two Braak I cases used for DSP analysis were excluded from the neuronal quantification because the tissue physically damaged or the ROI was not available entirely, a prerequisite for quantification. Image magnification was corrected by the embedded scale bar if the exported DSP images have different scale. Insoluble tau population was quantified using semi-quantification methods. The same slides performed DSP analysis were re-scanned using Axioscan 7 (Carl Zeiss AG, Oberkochen, Germany) to quantify the insoluble tau. Data consistency in counts were confirmed between two trained, blinded investigators.

Results

The number of neuromodulatory neurons in the suprachiasmatic nucleus start to progressively decrease in size from Braak stage II onwards

The changes of SCN neurons are depicted in Figure 3. The total number of AVP+ and VIP+ neurons decreased in AD progressive stages. At Braak VI cases, the mean number of neurons were 50% smaller compared to Braak 0 cases. Interestingly, at Braak II, the SCN neuronal number was already ~40% smaller than Braak 0 cases, showing the AD related changes in SCN precedes the bulk of cortical changes in AD.

Suprachiasmatic nucleus is more susceptible to accumulate phospho-tau than amyloid beta

Elevated pathological tau accumulation was confirmed by both histological examination and digitally quantified proteomics (Figure 4). Neurofibrillary tangles and insoluble tau accumulations in AD were predominantly examined in the SCN and the adjacent hypothalamic region (surrounding of the SCN) compared to the neighboring nuclei, PVN and SON (Figure 4a). DSP based measures of p-tau (p-S214, p-S396, and p-S404) levels were significantly elevated in AVP+ neurons already at Braak II. However, Aß levels were only detected at Braak VI cases (Figure 4b). Aligned with these findings regarding soluble proteins, neuropathological analysis with immunohistochemistry reveled NFT in SCN but not plaques, even at Braak VI (Figure 4a, c). In contrast, the neighboring nuclei expressing AVP+, i.e PVN and SON, only showed significant changed in p-tau level at Braak VI and the PVN also showed increases in beta-amyloid level at Braak VI only (Figure 4b).

Glial proteins are dysregulated in the SCN neurons before the advent of p-tau pathology

Figure 5 presents the DEP analyses of 36 cellular and subcellular markers involved in AD pathogenesis, within the SCN at progressive AD stages (Figure 5a) and conducted at SON and PVN (Figure 5b). Astrocytic glial markers, GFAP and S100B were significantly detected to the SCN AVP+ neurons even before increases in soluble p-tau burden was detected. Interestingly, the upregulated astroglia related proteins diminished in late AD stages. Microglial related proteins show dysregulation throughout AD progression. For instance, we detected a reduction in the level of P2RY12, which is a homeostatic microglial interaction involved in misfolded protein phagocytosis. Moreover, the altered microglial phagocytic properties found by the reduced CD11b+/CD45+ across the AD progression, showing an association with increasing insoluble NFT population in the SCN. The altered glial profile, observed in the SCN even in Braak I, whereas it was absent in the AVP+ neurons in the PVN. Interestingly, P2RY12+ protein co-localized to the SON neuron was significantly decreased compared to the Braak 0, remaining a question about its endogenous expression level in the non-pathological condition.

Discussion

The findings of this paper reveal the molecular and pathological changes occurring within the human SCN across the ADNC stages. These alterations have been underexamined in previous AD research. Utilizing DSP-based protein quantification specifically in SCN neurons, we identified the involvement of glial cells prior to ADNC progression. In the late stages of AD, NFTs were found selectively in the SCN, while also providing protection against amyloid plaques. This study emphasizes that the significance of understanding the vulnerability of both neurons and glial cells in the SCN to comprehend the circadian disorders observed in AD patients.

The etiology of AD is heterogeneous and involves multipathogenic and environmental changes (10). For this reason, the driving force behind the early susceptibility of the SCN pathology is controversial. However, there is evidence that hypothalamic nuclei and brainstem nuclei, which connect directly to the SCN and contribute to circadian-sleep-wake regulation, are vulnerable to tau-associated neurodegeneration in patients with Alzheimer's disease (11), leading to the neuronal death was associated with clinical sleep disturbances (12). Although it is a challenging to distinguish the neuronal basis matrix of abnormal circadian behavior and physiology from the multiple pathways of the metabolism, finding a direct association between the pathological changes in the SCN and circadian physiological abnormalities remains an exploration, suggesting the development of objective examination criteria for evaluating the circadian function.

Investigating SCN neuronal-specific susceptibility is also a crucial point. Preliminary research has revealed the SCN neuronal specific susceptibility is also crucial point to investigate. Preliminary research revealed that the loss of AVP+ neurons in the SCN identified in AD patients (7,13,14). AVP+ neurons through the PVN, which received the efferent signals from the SCN promote wake-promoting nuclei (15), and the neuronal activity in the SCN regulates clock gene expression and circadian behavior in animal model studies (16–18). Likewise, VIP+ neurons are essential to process light-mediated circadian cue (19,20), and degenerated in AD patients (6). Therefore, it supports our ongoing study, which involves a detailed anatomical analysis of the subregion of the SCN, focusing on the of AVP+ and VIP+ neurons.

The role of astrocyte in the SCN regulating circadian genes supports the increased astrocyte marker on the SCN neurons in the progression of ADNC (21–24). Further studies are required to validate the morphology and distribution of glial cells in the SCN. Selective vulnerability exhibited differential neuropathologic alterations between the SCN, PVN, and SON, prompting questions about the potential mechanisms underlying this alteration. Additionally, it raises a significance about the extent of association between each nucleus and other circadian/sleep/wake-promoting nuclei in the SCN circuitry (1,3).

Table 1. Demographic characteristics of participants

	Braak 0	Braak I	Braak II	Braak VI (Amnestic AD)
Total	12	12	6	11
Female, n (%)	3 (25%)	5 (42%)	3 (50%)	3 (27%)
Male, n (%)	9 (75%)	7 (58%)	3 (50%)	8 (73%)
Age of death, mean, yr (SD)	54 (3)	58 (6)	71 (8)	69 (8)
Disease onset, mean, yr (SD)	na	na	na	59 (9)

Figures

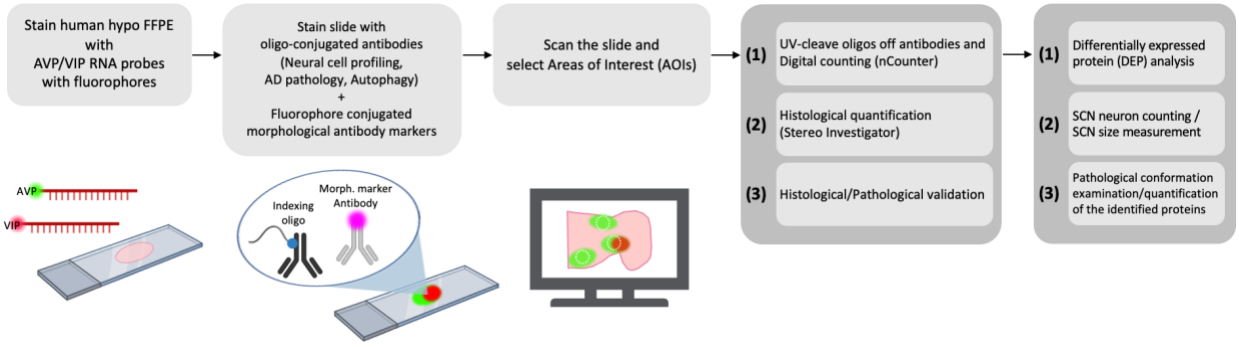

Figure 1. Experimental workflow.

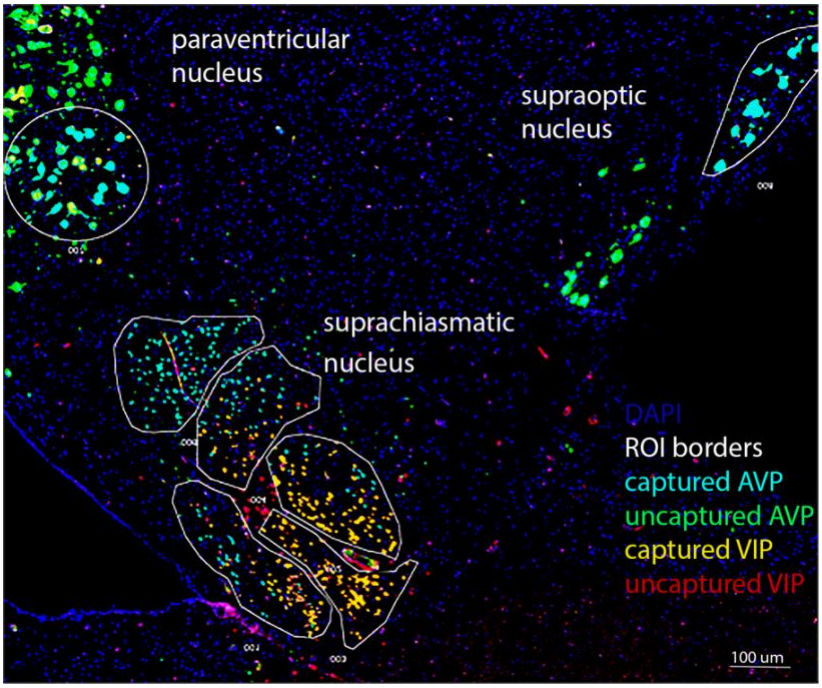

Figure 2. Representative AVP+ and VIP+ neurons in the SCN, PVN and SON.

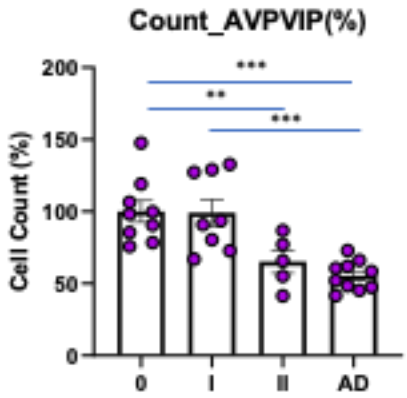

Figure 3. Histological quantification in the SCN. AVP+ and VIP+ neurons in SCN across Braak stages 0-II and Braak stage VI. Data was normalized by the mean of Braak stage 0. The purple dots indicate each individual subject. P-values were analyzed by *Wilcoxon* test (** $P < 0.01$, *** $P < 0.001$). Abbreviations: AVP; Arginine vasopressin, VIP; Vasoactive intestinal protein, AD; Alzheimer's Disease.

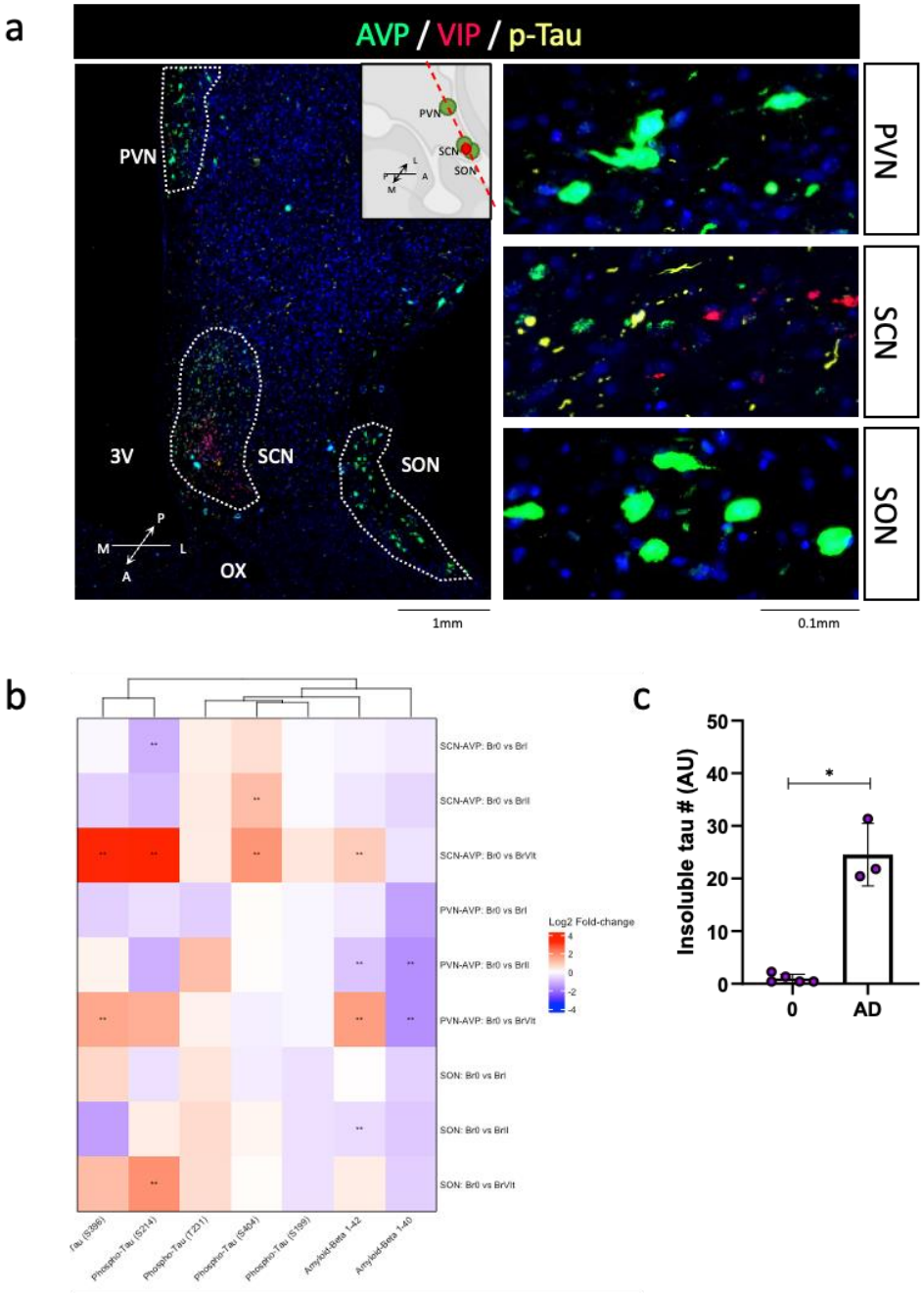

Figure 4. Digitally estimated differentially expressed AD hallmark proteins in the SCN, PVN, and SON in the progression of AD stages (normalized by DEP in Braak 0 cases (N=12))

(a) AVP and VIP-expressing neurons in the SCN and the neighboring nuclei using RNA fluorescence in-situ hybridization and p-Tau immunoreactivity. (Left) A coronal section of the anterior hypothalamus including the SCN and its neighboring nuclei, the PVN and SON. Scale bar: 1mm. (Left-right top) Illustration of hypothalamus with a view of sagittal plane indicating coronal section including the nuclei-of-interest. (Right) AVP (green) / VIP (red) / p-Tau (yellow) fluorescent signals in the PVN, SCN, and SON (from top to bottom). Scale bar: 0.1mm. Abbreviations: 3V; Third ventricle, A; anterior, AVP; arginine

vasopression, L; lateral, M; medial, OX; optic chiasm, P; posterior, PVN; paraventricular nucleus, SCN; suprachiasmatic nucleus, SON; supraoptic nucleus, VIP; vasoactive intestinal protein. (b) Comparison between differentially expressed proteins (DEP). Each row displays DEP in each Br compared to Br0. Log2 Fold-change values are color-annotated, with up-regulated proteins in red and down-regulated proteins in blue. A blue dashed square represents the DEPs in the SCN. Each column shows proteins quantified by the barcode. P-values were calculated using pseudobulk analysis including permutation test (** P < 0.01). (c) Comparison of AT8+ insoluble tau levels in Braak stage 0 and individuals with Braak VI. Data was normalized by average value in the Braak stage 0. P-value was calculated using the Wilcoxon test (* P < 0.05. Abbreviations: Br; *Braak* stage, PVN; paraventricular nucleus, SCN; suprachiasmatic nucleus, SON; supraoptic nucleus.

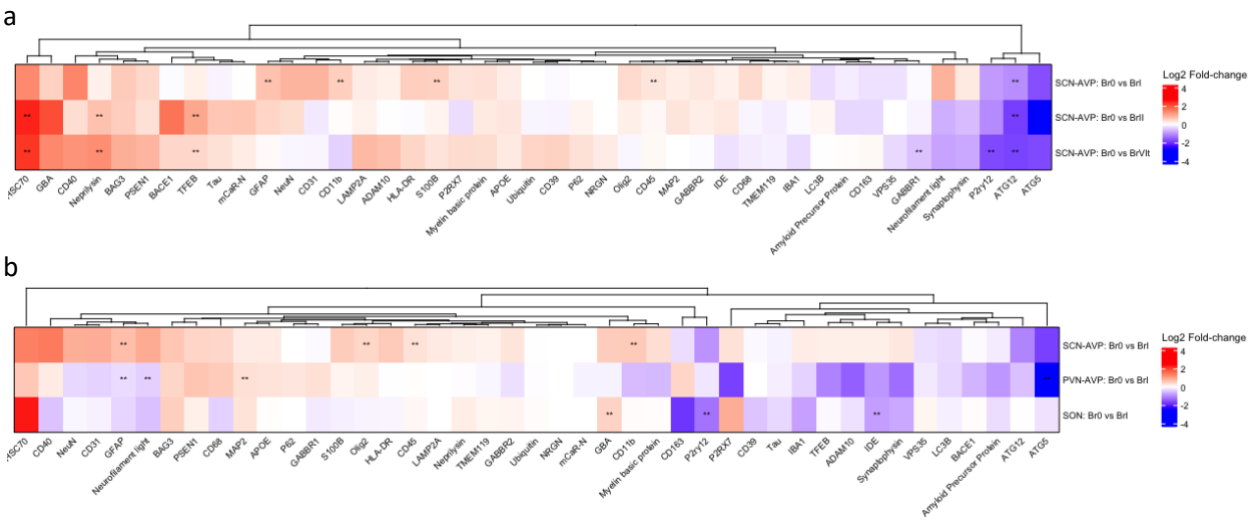

Figure 5. Digitally estimated differentially expressed pathological and cellular marker proteins in the SCN. **(normalized by DEP in Braak 0 cases (N=12))**

(a) Comparison between differentially expressed proteins (DEP) in the progressive ADNC stages. (b) Comparison between DEP between SCN, PVN, and SON in Braak stage I. Each row displays DEP in each Br compared to Br0. Log2 Fold-change values are color-annotated, with up-regulated proteins in red and down-regulated proteins in blue. A blue dashed square represents the DEPs in the SCN. Each column shows proteins quantified by the barcode. P-values were calculated using pseudobulk analysis including permutation test (** P < 0.01).

References

1. Son G, Neylan TC, Grinberg LT. Neuronal and glial vulnerability of the suprachiasmatic nucleus in tauopathies: evidence from human studies and animal models. Molecular Neurodegeneration. 2024 Jan 10;19(1):4.

2. Ehrenberg AJ, Kelberman MA, Liu KY, Dahl MJ, Weinshenker D, Falgàs N, et al. Priorities for research on neuromodulatory subcortical systems in Alzheimer's disease: Position paper from the NSS PIA of ISTAART. Alzheimer's & Dementia [Internet]. [cited 2023 Mar 16];n/a(n/a). Available from: https://onlinelibrary.wiley.com/doi/abs/10.1002/alz.12937

3. Lew CH, Petersen C, Neylan TC, Grinberg LT. Tau-driven degeneration of sleep- and wake-regulating neurons in Alzheimer's disease. Sleep Medicine Reviews. 2021 Dec;60:101541.

4. Thal DR, Rüb U, Orantes M, Braak H. Phases of A beta-deposition in the human brain and its relevance for the development of AD. Neurology. 2002 Jun 25;58(12):1791–800.

5. Braak H, Braak E. Neuropathological stageing of Alzheimer-related changes. Acta Neuropathol. 1991 Sep 1;82(4):239–59.

6. Zhou JN, Hofman MA, Swaab DF. VIP neurons in the human SCN in relation to sex, age, and Alzheimer's disease. Neurobiology of Aging. 1995 Jul 1;16(4):571–6.

7. Swaab DF, Fliers E, Partiman TS. The suprachiasmatic nucleus of the human brain in relation to sex, age and senile dementia. Brain Research. 1985 Sep 2;342(1):37–44.

8. Ono D, Honma KI, Honma S. Roles of Neuropeptides, VIP and AVP, in the Mammalian Central Circadian Clock. Front Neurosci. 2021;15:650154.

9. Dudás B. Part II - Hypothalamic coronal sections: Myelo- and Cytoarchitecture. In: Dudás B, editor. Atlas of the Human Hypothalamus [Internet]. Academic Press; 2021 [cited 2024 Mar 7]. p. 25–8. Available from: https://www.sciencedirect.com/science/article/pii/B978012822051100002X

10. Korczyn AD, Grinberg LT. Is Alzheimer disease a disease? Nat Rev Neurol. 2024 Feb 29;1–7.

11. Oh J, Eser RA, Ehrenberg AJ, Morales D, Petersen C, Kudlacek J, et al. Profound degeneration of wake-promoting neurons in Alzheimer's disease. Alzheimer's & Dementia. 2019;15(10):1253–63.

12. Oh JY, Walsh CM, Ranasinghe K, Mladinov M, Pereira FL, Petersen C, et al. Subcortical Neuronal Correlates of Sleep in Neurodegenerative Diseases. JAMA Neurology. 2022 May 1;79(5):498–508.

13. Wu YH, Zhou JN, Van Heerikhuize J, Jockers R, Swaab DF. Decreased MT1 melatonin receptor expression in the suprachiasmatic nucleus in aging and Alzheimer's disease. Neurobiology of Aging. 2007 Aug 1;28(8):1239–47.

14. Harper DG, Stopa EG, Kuo-Leblanc V, McKee AC, Asayama K, Volicer L, et al. Dorsomedial SCN neuronal subpopulations subserve different functions in human dementia. Brain. 2008 Jun;131(Pt 6):1609–17.

15. Islam MT, Rumpf F, Tsuno Y, Kodani S, Sakurai T, Matsui A, et al. Vasopressin neurons in the paraventricular hypothalamus promote wakefulness via lateral hypothalamic orexin neurons. Current Biology. 2022 Sep 26;32(18):3871-3885.e4.

16. Buijs RM, Hurtado-Alvarado G, Soto-Tinoco E. Vasopressin: An output signal from the suprachiasmatic nucleus to prepare physiology and behaviour for the resting phase. J Neuroendocrinol. 2021 Jul;33(7):e12998.

17. Dzirbikova Z, Kiss A, Okuliarova M, Kopkan L, Cervenka L. Expressions of per1 clock gene and genes of signaling peptides vasopressin, vasoactive intestinal peptide, and oxytocin in the suprachiasmatic and paraventricular nuclei of hypertensive TGR[mREN2]27 rats. Cell Mol Neurobiol. 2011 Mar;31(2):225–32.

18. Nicola AC, Ferreira LB, Mata MM, Vilhena-Franco T, Leite CM, Martins AB, et al. Vasopressinergic Activity of the Suprachiasmatic Nucleus and mRNA Expression of Clock Genes in the Hypothalamus-Pituitary-Gonadal Axis in Female Aging. Front Endocrinol (Lausanne). 2021;12:652733.

19. Jones JR, Simon T, Lones L, Herzog ED. SCN VIP Neurons Are Essential for Normal Light-Mediated Resetting of the Circadian System. J Neurosci. 2018 Sep 12;38(37):7986–95.

20. Mazuski C, Abel JH, Chen SP, Hermanstyne TO, Jones JR, Simon T, et al. Entrainment of Circadian Rhythms Depends on Firing Rates and Neuropeptide Release of VIP SCN Neurons. Neuron. 2018 Aug;99(3):555-563.e5.

21. Brancaccio M, Patton AP, Chesham JE, Maywood ES, Hastings MH. Astrocytes Control Circadian Timekeeping in the Suprachiasmatic Nucleus via Glutamatergic Signaling. Neuron. 2017 Mar 22;93(6):1420-1435.e5.

22. Brancaccio M, Edwards MD, Patton AP, Smyllie NJ, Chesham JE, Maywood ES, et al. Cell-autonomous clock of astrocytes drives circadian behavior in mammals. Science. 2019 Jan 11;363(6423):187–92.

23. Coomans C, Saaltink DJ, Deboer T, Tersteeg M, Lanooij S, Schneider AF, et al. Doublecortin-like expressing astrocytes of the suprachiasmatic nucleus are implicated in the biosynthesis of vasopressin and influences circadian rhythms. Glia. 2021 Nov;69(11):2752–66.

24. Marpegan L, Krall TJ, Herzog ED. Vasoactive intestinal polypeptide entrains circadian rhythms in astrocytes. J Biol Rhythms. 2009 Apr;24(2):135–43.